

A Multi-stage Hierarchical Approach to Alloy Design

P.K. Ray, T. Brammer, Y.Y. Ye, M. Akinc, and M.J. Kramer

A multi-stage hierarchical sieving approach based on a combination of semi-empirical and ab initio calculations along with selected experimental studies was used to down-select potential alloy systems for ultra-high-temperature applications. This approach indicates that the Mo-Ni-Al system has potential for applications at the target temperatures of 1,200–1,300°C. The Mo was selected for its high melting temperature, room temperature toughness, and creep resistance while the NiAl is a reservoir for the Al₂O₃ passivating scale. Microstructures based on casting and powder processing of the Mo-Ni-Al alloys were studied. Oxidation behavior of the Mo-Ni-Al alloys at 1,100 and 1,200°C in dry air was determined and those alloys with ≤20 at.% Mo were shown to be superior to the T2 (Mo₅SiB₂). Furthermore, the calculations predicted that small amounts of platinum group metals Pd, Ir, and Rh additions would increase the melting temperature without forming detrimental intermetallic phases, which results in improved oxidation stability of the NiAl phase.

INTRODUCTION

Superalloys are the workhorse materials for land-based gas turbine blades, which are required to operate under extremely harsh combustion environments while retaining their mechanical integrity. Operating temperatures for Ni-based superalloys have been greatly increased by application of the thermal barrier coating along with a suitable Ni-Al-based bond coat. Commercial turbine blades are routinely operated at temperatures up to 1,150°C.¹ Even higher efficiencies such as envisioned in the U.S. Department of Energy (DOE) National Energy Technology Laboratory's FutureGen gas turbine program will

How would you...

...describe the overall significance of this paper?

Discovery of new alloys that can operate at temperatures well above Ni-based superalloys requires new and more efficient means of sifting through prospective phase space. We present a semi-empirical approach combined with more accurate computational materials design, density functional theory, to rapidly identify a prospective alloy for ultra-high-temperature applications.

...describe this work to a materials science and engineering professional with no experience in your technical specialty?

Traditional materials discovery involves researcher's basic materials: knowledge, intuition and a lot of trial and error. The semi-empirical approach used here allows us to estimate formation enthalpies as a rapid screening method to identify regions in ternary systems that have high melting temperatures. In this way we can screen thousands of combinations in a short time. We then use more accurate ab initio methods to refine our search.

...describe this work to a layperson?

The maximum operating temperature of current commercial Ni-based superalloys is ~1,150°C. However, the objectives of the FutureGen project require alloys that can function at about 1,350°C. Such large increases in operating temperatures will require new materials. An Edisonian approach to the discovery of new materials is tedious and we lack the numerical tools to efficiently predict new phases. For instance, a four-component Ni-based system, with all elements selected from the transition metals, leads to 3,654 possible combinations, while Ni-based superalloys may have eight elements or more. A rapid means of 'sieving' through possible combinations of elements is presented.

require alloys that can function at temperatures above the melting point of today's commercial alloys. Hence, design of ultra-high-temperature alloys will require a major breakthrough. Refractory metal silicides in the metal-T2-A15 phase field region can operate at high temperatures and retain their strength.^{2–5} However, the oxidation resistance of these alloys is significantly reduced. Alloys in the T1-T2-A15 or disilicides of refractory metals offer improved oxidation resistance.⁶ However, the presence of only brittle intermetallics in the phase assemblage renders them unusable in practice.

A significant increase in operating temperatures is not likely to be achieved by tweaking current Ni-based alloy compositions. A trial-and-error based approach toward the discovery of new materials is tedious, yet we lack the numerical tools to efficiently and accurately predict new phases and their properties. Potential phase space is enormous. For instance, a four-component Ni-based system, with all the elements selected from the transition metal elements, yields 3,654 possible combinations, and adding only one more constituent expands the number of combinations to 23,751. Considering that many commercial high-temperature alloys can have in excess of eight constituents, a systematic investigation of even a fraction of the potential phase space through computational thermodynamics or *ab initio* methods is unrealistic. Hence using rapid sieving techniques in an alloy design project is essential. Faster but lower accuracy approaches to quickly screen out the least favorable combinations followed by more rigorous methods to narrow the potential phase space offers an efficient alloy design approach.

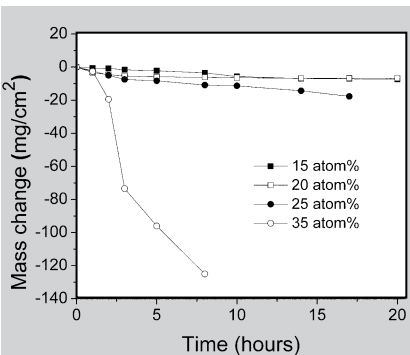


Figure 1. Interrupted flowing air oxidation of liquid phase sintered alloys of different Mo content at 1,100°C.

Fortunately, we do have a few clues to pursue for developing fast screening methods. For instance, the melting temperature of a material can be taken as one of the guidelines for a prospective high-temperature alloy. The melting temperature of a compound, in turn, correlates well with the interatomic bond strength and its formation enthalpy.^{7–9} It has been demonstrated that the formation enthalpy of a multicomponent system can be estimated with a reasonable degree of accuracy and extremely low computational cost using an extended Miedema approach.¹⁰ However, melting temperature is not the only requirement; only certain elements are known to promote the formation of protective oxide scales, most notably, Al, Cr, and Si. Therefore, additional screening criteria include developing alloys comprised of a phase that will promote the formation of a slow-growing protective oxide scale. Due to the low stability of chromia at the target operating temperatures, 1,350°C, and susceptibility of silica-based scales to moisture in coal combustion byproducts, we are left with an alumina-forming alloy.¹¹ Alloys based on a mix of refractory metals (RM) and NiAl are believed to be the best candidates. The RM forms the backbone of the alloy, providing toughness at low temperatures and creep resistance at high temperatures. The β -NiAl (B2 structure, SG 221), in turn, acts as a reservoir for the passivating alumina scale. However, alloying additions to the NiAl are required in order to boost its melting temperature ($T_m = 1,640^\circ\text{C}$).

The primary focus of this study was to evaluate a series of alloy combinations narrowed down by the guidelines mentioned above, using semi-empirical, as well as *ab initio* calculations for

their potential as a high temperature ($T \sim 1,300^\circ\text{C}$), oxidation and fracture resistant material. Select alloy compositions predicted by the computational tools were then synthesized, characterized, and tested for their high-temperature oxidative stability as the first goal-post in the alloy development process.

THEORETICAL CALCULATIONS

The initial cut through the prospective phase space was performed using semi-empirical calculations based on an extended Miedema approach.¹⁰ Briefly, this approach is based on using an energy minimization scheme by optimizing the compositions of the constituent binary systems under appropriate mass balance constraints. Our modified Miedema model was used for estimating the difference in formation enthalpies between NiAl and TM-Al (TM = transition metal). Twenty-six elements from the transition metal block were tested over the entire composition range of their ternaries with Ni and Al. Three considerations were given for the selection of the TM: high formation enthalpy, absence of intermetallics with Ni or Al over a significant composition range, and a cubic crystal form to insure some ductility at lower temperatures. Using these criteria, Mo was clearly the best candidate. Molybdenum retains its body-centered cubic (bcc) structure up to its melting temperature and has a limited solubility with Al or Ni. While not possessing good oxidation stability of itself, its low diffusivity and low solubility with NiAl suggests that a graded microstructure can be designed to minimize susceptibility for oxidation.

The next step in alloy design was to search for ternary addition to the NiAl to boost its melting temperature. As mentioned above, the ternary additions to the NiAl should not only raise the melting temperature but should be retained in solid solution with the NiAl. Again we used our modified Miedema model to down-select the most promising candidates based on their formation enthalpies. Of the late-transition elements, only Hf, Y, Zr, Nb, Pd, Rh, and Ir showed the highest formation enthalpies with NiAl and a smaller affinity for Mo. It is critical that the ternary addition to NiAl does not exhibit high heat of mix-

ing with Mo. At this point, more accurate calculations were required.

Ab initio methods are preferred at this stage. Unlike embedded atom methods, interatomic potentials do not have to be developed or in the case of computational thermodynamics, developing databases are not necessary. The disadvantage of *ab initio* methods is in instances where the crystal structure and its atomic decoration are not known so that a large number of prospective structures must be calculated. It should be stressed that unless specifically determined, *ab initio* provides only the most enthalpically stable structure (0 K). Entropically stable structures or highly complex low symmetry systems are very difficult to identify with this approach. In this particular system we suspected that the small platinum group metal (PGM) additions will not result in degeneracy of the β -NiAl, which was readily confirmed experimentally. Therefore the number of calculations required was small.

The *ab initio* calculations were carried out using the Vienna *ab initio* Sim-

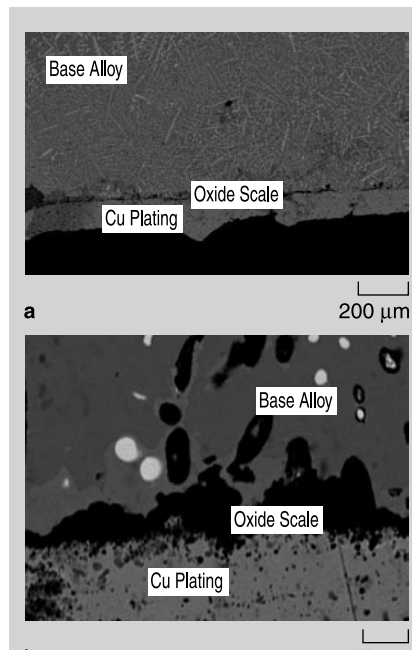


Figure 2. (a) Low magnification image of the oxidized alloy. The alumina scale appears to have formed continuously on the surface. (b) Higher magnification image of the oxidized alloy showing the non-uniformity of scale thickness primarily as a result of presence of Mo phase at the surface. Mo gets oxidized and the resultant MoO_3 volatilizes allowing oxygen to penetrate relatively larger distances into the alloy.

ulation Package (VASP)^{12–14} to get the thermodynamically stable structure of B2 phase in the $\text{Ni}_{1-x}\text{AlTM}_x$ and $\text{NiAl}_{1-x}\text{TM}_x$ systems using a 54-atom supercell, where TM represents the transition metal element selected by the Miedema's model. The density functional calculations are performed using a plane-wave pseudo-potential representation, with ultra-soft pseudo-potentials¹³ for all species and with a plane-wave energy cutoff of 300 eV. The k-point sampling was chosen to converge all of the total energies to an accuracy of 2 meV/atom. The k-point grid used for structural relaxation was $6\times 6\times 6$, chosen according to the Monkhorst-Pack scheme,¹⁵ and symmetry reduced to the irreducible Brillouin zone.

See the sidebar for experimental methods.

RESULTS AND DISCUSSION

Oxidation Behavior of the Mo-Ni-Al Alloys

Samples processed by liquid phase sintering showed the influence of alloy composition on the oxidation behavior. Alloys under 20 at.% Mo, with equiatomic NiAl showed fairly good oxidation resistance, while the alloys with a higher volume fraction of Mo (e.g. $\text{Mo}_{35}\text{Ni}_{32.5}\text{Al}_{32.5}$) failed to form a passivating oxide layer (Figure 1). The strong composition dependence of oxidation is due to Mo's deleterious effect on the oxidation resistance. Minimizing the interconnected Mo network is required. Continuity of Mo phase depends on its volume fraction and the size of the Mo grains. The higher the volume fraction of the Mo phase and larger the grain size, the larger is the probability of connectivity, resulting in poorer oxidation resistance.

Figure 2a shows a low-magnification microstructure of the oxidized $\text{Mo}_{20}\text{Ni}_{40}\text{Al}_{40}$ cast alloy at 1,200°C. It can be seen that the alloy has developed a continuous alumina scale of about 5 μm thickness, albeit not uniform, across the length of the sample. A look at the oxide scale at higher magnification (Figure 2b) shows that the scale thickness fluctuation is due to the presence of long Mo dendrites growing into the alloy.

It has been widely observed in Ni-based alloys that the initial oxidation

EXPERIMENTAL METHODS

Based on our calculations, the Mo-Ni-Al system was selected as a viable candidate for the base alloy. A number of compositions in this system were tested for their resistance to high temperature oxidation. The testing temperatures were restricted to 1,200°C due to massive scale spallation at higher temperatures. This pointed to a need for improving the NiAl phase with selected transition metal additions as indicated by the calculations above.

Mo-Ni-Al Alloys

Mo-Ni-Al alloys are known to exhibit a two-phase (bcc Mo + β-NiAl) microstructure over a limited range of compositions.¹⁶ All the experiments in the present study were carried out in this phase field. Higher phase fraction of molybdenum would be detrimental to the oxidation resistance; hence the phase fraction of Mo was kept below 35 at.% in all cases. The alloys were synthesized using powder metallurgical techniques as well as casting. The powder metallurgy involved mixing the pure metal powders (~10 μm) in a mixer/shaker (SPEX 8000, SPEX CertiPrep Inc, Metuchen, NJ) for 10 min. followed by compaction of the powders by dry pressing at a pressure of 24 MPa. The cylindrical pellets thus produced had a diameter of 10 mm and a height of 20 mm. The pellets were then sintered at 1,750°C for 45 min. The pellets synthesized by this route had nominal compositions of Mo = 15, 20, 25, and 35 at.%, with the balance in each case being equiatomic NiAl. Oxidation coupons having a diameter of 10 mm and a thickness of 1 mm were cut from the cylindrical samples and subjected to interrupted oxidation tests at 1,100°C which is the maximum temperature that current superalloys are exposed to in practice. Oxidation tests with multiple compositions allowed us to study the effect of Mo phase fraction and determine an appropriate composition range where the oxidation resistance was reasonably optimized.

The composition of the drop-cast alloy ($\text{Mo}_{20}\text{Ni}_{40}\text{Al}_{40}$) was decided based on the oxidation behavior of the sintered alloys. Drop-cast samples were prepared from pelletized elemental powder mixture of Mo (Alfa Aesar, 99.5% purity), Ni (MPC, 99.6% purity) and Al (Alfa Aesar, 99.8% purity) which were arc-melted. The alloys were re-melted thrice to achieve a greater degree of homogenization followed by drop-casting in order to obtain a cylindrical rod. The drop-cast alloy was subject to interrupted oxidation tests over a range of temperatures from 1,000°C to 1,200°C.

In this test, the samples were exposed to the target temperatures for a total of 20 h with occasional interruptions for mass measurements at ambient temperature. The testing temperatures were deliberately kept at 1,200°C or lower since our work on oxidation of pure nickel aluminides at temperatures above 1,200°C (discussed below) has shown massive scale spallation. Microstructures of the as-prepared alloys as well as the oxidized coupons were studied using a JEOL 5910LV scanning electron microscope (JEOL, Tokyo, Japan) at an accelerating voltage of 20 kV.

Nickel Aluminides with TM Additions

The Ni-Al-TM alloys were produced from pieces cut from pure bulk metal sheets obtained from the Materials Preparation Center at Ames Laboratory, having a purity of 99.7% or more. Pure Ni and Al were first arc-melted together in an argon atmosphere to form β-NiAl. The ab initio calculations suggested that the transition metals have a preference for the Ni site in the B2 structure. Alloys with compositions $\text{Ni}_{50-x}\text{Al}_{50}\text{TM}_x$ (x = 3, 6, and 9) were then arc-melted in an argon atmosphere. The samples were re-melted thrice to achieve better homogenization before drop-casting. The rods were annealed at 1,300°C in an argon atmosphere for 6 h to ensure homogeneity. Scanning electron microscopy was used to characterize the microstructure while phase analysis was done using x-ray diffraction (XRD) on a Philips PANalytical x-ray diffractometer (Panalytical, Almelo, Netherlands) with a Bragg-Brentano geometry and Cu K α_1 radiation ($\lambda = 1.54056 \text{ \AA}$). The x-ray data was Rietveld refined using GSAS software to estimate the lattice parameters of the phases as well as determine site preference for different elements.¹⁷ Of the transition metals studied, alloys with platinum group metal (PGM) modifications formed single phase alloys while the other alloys showed a eutectic microstructure. Hence, further studies were carried out only on the PGM modified alloys. Oxidation coupons were prepared as described above, but more aggressive testing conditions, 1,300°C for two hours and ambient for 30 min, were employed to determine if the PGM improved the oxidation stability of NiAl reservoir phase.

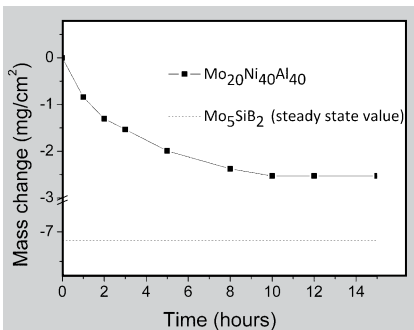


Figure 3. Interrupted flowing air oxidation of an arc-melted and drop cast alloy ($\text{Mo}_{20}\text{Ni}_{40}\text{Al}_{40}$) at 1,200°C.

product of NiAl is the formation of NiO .¹⁸ Subsequently, NiO is reduced by Al resulting in the formation of Ni and Al_2O_3 . Typically such a reduction results in linear rather than parabolic kinetics. Aluminum can also react with atmospheric oxygen to form Al_2O_3 which should exhibit parabolic oxidation kinetics. Additionally, NiO and Al_2O_3 can react to form an NiAl_2O_4 spinel.¹⁹ All the reactions involving Ni and Al result in a slow mass gain, whereas the oxidation of Mo and the subsequent volatilization of MoO_3 results in a rapid mass loss.⁴ Consequently, the overall oxidation rate is a sum of mass gain due to oxidation of Ni and Al and loss due to volatilization of MoO_3 . Figure 3 shows the oxidation kinetics during the interrupted oxidation process for the $\text{Mo}_{20}\text{Ni}_{40}\text{Al}_{40}$ alloy at 1,200°C. As a baseline comparison, the steady state mass loss value for the T2- Mo_5SiB_2 compound is shown on the same figure for comparison. The preliminary data indicates that the oxidation behavior of Mo-Ni-Al alloy is comparable to the refractory metal silicides at fairly elevated temperatures.

Oxidation studies were limited to a temperature of 1,200°C because the alumina scale formed on nickel aluminides is prone to spallation above 1,200°C.

Oxidation Behavior of the Nickel Aluminide

X-ray diffraction studies on the nickel aluminides with Zr, Y, Hf, and Nb additions indicated a two phase mixture. The PGM additions were shown to form a single phase with the same crystal system as the β -NiAl. A monotonic and approximately linear increase in the lattice parameter was observed with increasing PGM additions. Sub-

sequent Rietveld refinement confirmed that PGM substitutions preferred the Ni site, which is in accordance with the *ab initio* calculations (Figure 4).

Figure 4 shows the variation of formation enthalpy of PGM substituted β -NiAl. It can be seen that substitution of PGM elements for Ni is energetically favorable. Also, controlled additions result in a monotonic change in formation enthalpy. This suggests that these PGM additions might be beneficial for obtaining an increase in the melting temperature of the nickel aluminide. The other transition metals that showed large negative formation enthalpies with the nickel aluminide included Hf, Y, Zr, and Nb. All of these additions were experimentally found to produce deep eutectics. A high formation enthalpy can indicate high stability of both the solid and the liquid phase. The phase selection is decided by the relative stability of these two phases. Miedema's model is a structureless model; hence it can't be used to predict which of these two phases will be more stable. Formation of a eutectic suggests that the liquid phase is relatively more stable compared to a single phase intermetallic with the same composition in case of these alloying additions. Hence, further oxidation studies were carried out with only the PGM additions, since they were readily soluble in the β -NiAl.

Figure 5 shows the oxidation kinetics for the three PGM substitutions (all 6 at.%) to the β -NiAl compared against undoped β -NiAl as a benchmark. It can clearly be seen that the Pd substitution performed worse than the β -NiAl during oxidation testing at 1,300°C. The oxide spallation of the Pd sample was

noticeable early on during the test. The spallation flakes were large and discernible with the naked eye, just like the β -NiAl spallation. The Rh sample performed better than the base alloy NiAl, but worse than the alloy doped with Ir. The sample with Rh showed an adherent oxide scale initially, but after five hours oxide spallation was observed. From the oxidation resistance point of view, Ir substitution to β -NiAl appears to be superior. No sign of spallation was evident at times shorter than 20 h for alloys with 9 at.% substitution. In all cases it should be noted that the best performing alloy at the end of 20 h was always the alloy with the highest fraction of the ternary substitution for all of the elements tested.

Figure 6a-d shows the oxidation microstructures of the baseline NiAl along with each ternary substitution set at 6 at.%. These samples were oxidized for 24 h at 1,300°C and then examined to better assess the evolution of the oxide scale formation. Figure 5 clearly displays that neither the benchmark β -NiAl alloy nor the β -NiAl doped with Pd additions show an adherent oxide layer. Since both alloys had relatively significant mass loss, the surface would be devoid of a continuous oxide scale. The Rh doped β -NiAl showed an overall mass gain as well as signs of spallation. Looking at the oxide microstructure, it can be seen that the oxide layer is fairly continuous with a thickness of approximately 10 μm . The Ir addition showed an almost continuous oxide scale with a thickness of 8 μm . The only discontinuities were observed at the corners of the specimen where stresses in the oxide layer would be highest.

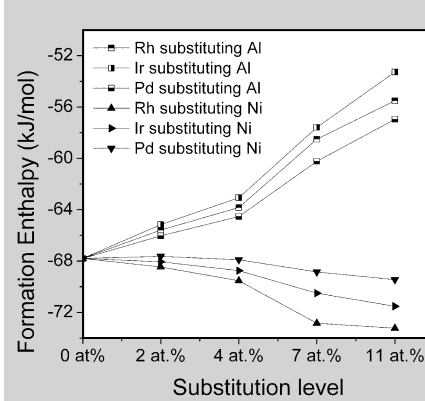


Figure 4. Variation of formation enthalpy of β -NiAl with PGM additions.

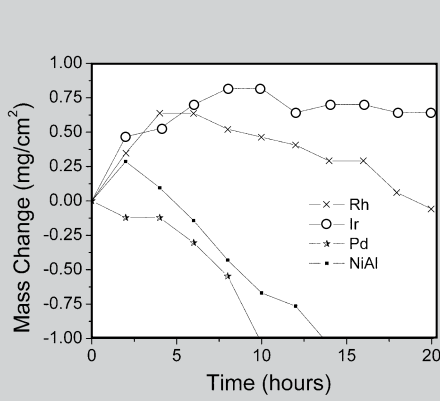


Figure 5. Cyclic oxidation of β -NiAl with and without PGM substitutions at 1,300°C.

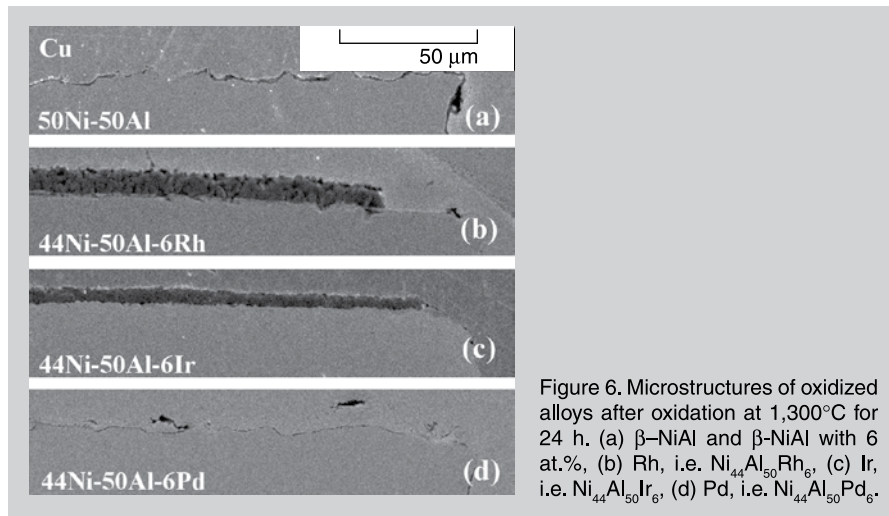


Figure 6. Microstructures of oxidized alloys after oxidation at 1,300°C for 24 h. (a) β -NiAl and β -NiAl with 6 at.%, (b) Rh, i.e. $\text{Ni}_{44}\text{Al}_{50}\text{Rh}_6$, (c) Ir, i.e. $\text{Ni}_{44}\text{Al}_{50}\text{Ir}_6$, (d) Pd, i.e. $\text{Ni}_{44}\text{Al}_{50}\text{Pd}_6$.

CONCLUSIONS

We have shown that a hierarchical approach to alloy design starting with a less accurate but fast tool, followed by a more accurate but time consuming computational tool can be an efficient and effective means of down-selecting high-temperature alloys. Our modified Miedema model is particularly effective in identifying regions of high (negative) formation enthalpies, indicative of high melting temperatures. Using the criteria of refractory base metal as the backbone of the alloy and identifying the NiAl as the most promising reservoir compound for alumina scale former, we demonstrated that Mo-Ni-Al-(PGM) shows good promise as a high-temperature alloy. To further stabilize the reservoir compound, the most enthalpically stable

ternary additions were determined. The most promising of the Ni-Al-(PGM) alloys based on *ab initio* calculations were synthesized and their oxidation behavior was studied. It was found that a few alloys in this system had enough potential to warrant further investigation of these materials for ultra-high-temperature applications. The Mo phase fraction and its grain size play a critical role in the oxidation behavior of these alloys. Future work would be focused on developing PGM substituted Mo-Ni-Al alloys in the two phase bcc-Mo(ss) + β -NiAl phase fields.

ACKNOWLEDGEMENT

This work was supported by the Department of Energy-Fossil Energy (Atmospheric Radiation Measurement program) through Ames Laboratory con-

tract no. DEAC02-07CH11358 through Iowa State University.

References

- R.C. Reed, *The Superalloys: Fundamentals and Applications* (Cambridge, U.K.: Cambridge University Press, 2006).
- M. Meyer, M. Kramer, and M. Akinc, *Adv. Mater.*, 8 (1996), pp. 85–88.
- M.K. Meyer, M.J. Kramer, and M. Akinc, *Intermetallics*, 4 (1996), pp. 273–281.
- M.K. Meyer and M. Akinc, *J. Amer. Cer. Soc.*, 79 (1996), pp. 938–944.
- J.R. Nicholls, *MRS Bulletin*, 28 (2003), pp. 659–670.
- A.J. Thom, E. Summers, and M. Akinc, *Intermetallics*, 10 (2002), pp. 555–570.
- J.H. Rose, J. Ferrante, and J.R. Smith, *Phys. Rev. Lett.*, 47 (1981), p. 675.
- C. Li and P. Wu, *Chem. of Mater.*, 14 (2002), pp. 4833–4836.
- C. Li, J. Lim Hoe, and P. Wu, *J. Phys. and Chem. of Solids*, 64 (2003), pp. 201–212.
- P.K. Ray, M. Akinc, and M.J. Kramer, *J. Alloys and Comp.*, 489 (2010), pp. 357–361.
- J.E. Croll and G.R. Wallwork, *Oxidation of Metals*, 4 (1972), pp. 121–140.
- G. Kresse and J. Furthmüller, *Phys. Rev. B*, 54 (1996), p. 11169.
- G. Kresse and J. Furthmüller, *Computational Mater. Sci.*, 6 (1996), pp. 15–50.
- G. Kresse and J. Hafner, *Phys. Rev. B*, 47 (1993), p. 558.
- H.J. Monkhorst and J.D. Pack, *Phys. Rev. B*, 13 (1976), p. 5188.
- X. Lu, Y. Cui, and Z. Jin, *Metal. and Mater. Trans. A*, 30 (1999), pp. 1785–1795.
- B.H. Toby, *J. Appl. Cryst.*, 34 (2001), pp. 210–213.
- G.R. Wallwork, *Reports on Progress in Physics*, 39 (1976), pp. 401–485.
- X. Zhao, I.P. Shapiro, and P. Xiao, *Surface and Coatings Technology*, 202 (2008), pp. 2905–2916.

P.K. Ray, T. Brammer, Y.Y. Ye, M. Akinc, and M.J. Kramer are with Ames Laboratory and Department of Materials Science and Engineering, Iowa State University, Ames, IA 50011. Dr. Kramer can be reached at mjkramer@ameslab.gov.

M. Akinc and M.J. Kramer are full TMS Members and T. Brammer is a student member!

To read more about them, turn to page 7. To join TMS, visit www.tms.org/Society/Membership.aspx.

TMS